



Crystal and electronic structure of the new quaternary sulfides $\text{TlLnAg}_2\text{S}_3$ ($\text{Ln} = \text{Nd}, \text{Sm}$ and Gd)



Abdeljalil Assoud, Yixuan Shi, Quansheng Guo, Holger Kleinke*

Department of Chemistry and Waterloo Institute for Nanotechnology, University of Waterloo, Waterloo, ON, Canada N2L 3G1

ARTICLE INFO

Keywords:

Sulfide
Chalcogenide
Crystal structure
Electronic structure

ABSTRACT

The quaternary sulfides $\text{TlLnAg}_2\text{S}_3$ ($\text{Ln} = \text{Nd}, \text{Sm}$ and Gd) were prepared via solid state reactions by heating the elements in the stoichiometric ratio under exclusion of air up to 750 °C. They are isostructural, adopting a new structure type in the space group $Pnma$ with $a = 13.8141(3)$ Å, $b = 4.1649(1)$ Å, $c = 11.4008(2)$ Å, $V = 655.94(2)$ Å³, $Z = 4$ for $\text{TlNdAg}_2\text{S}_3$. The crystal structure contains AgS_4 tetrahedra and LnS_6 octahedra, which are interconnected to form linear chains running along the b axis. The melting point of $\text{TlNdAg}_2\text{S}_3$ was determined to be 540 °C. Electronic structure calculations show that these materials are semiconductors in agreement with their orange/yellow colors.

1. Introduction

Various thallium chalcogenides have been investigated for usage as X- and γ-ray detectors [1–3] and in the thermoelectric energy conversion [4,5]. In both cases, the high atomic number and thus weight of thallium are advantageous, while - among other properties - a low electrical conductivity is beneficial for these detectors [6], and a low thermal but high electrical conductivity for thermoelectrics [7]. Therefore, typically the sulfides are more suitable as detectors because of their lower electrical conductivity, and the tellurides as thermoelectrics because of their higher electrical conductivity. With this in mind, we have investigated various thallium chalcogenide systems, discovering a variety of new materials in part adopting novel crystal structures such as Tl_2ZrTe_3 [8], Tl_4MTe_4 ($M = \text{Zr}, \text{Hf}$) [9], Tl_4MQ_4 [10], Tl_2MQ_3 [11] and Tl_2PbMQ_4 [12] (all with $M = \text{Zr}, \text{Hf}$ and $Q = \text{S}, \text{Se}$), $\text{Tl}_{18}\text{Pb}_2\text{M}_7\text{Q}_{25}$ ($M = \text{Ti}, \text{Zr}, \text{Hf}; Q = \text{S}, \text{Se}$) [13], and most recently $\text{Tl}_2\text{NdAg}_3\text{Q}_4$ ($Q = \text{Se}, \text{Te}$) [14]. In all of these cases, the sulfides and selenides were isostructural, while the tellurides could either not be synthesized, as in Tl_2PbMQ_4 and $\text{Tl}_{18}\text{Pb}_2\text{M}_7\text{Q}_{25}$, or adopted different structures, such as in Tl_2MQ_3 , Tl_4MQ_4 and $\text{Tl}_2\text{NdAg}_3\text{Q}_4$. Our attempts to prepare the sulfur analogue to $\text{Tl}_2\text{NdAg}_3\text{Se}_4$ or $\text{Tl}_2\text{NdAg}_3\text{Te}_4$ were not successful, but our expanded investigations surprisingly revealed a different sulfide with the same metal atoms, namely $\text{TlNdAg}_2\text{S}_3$. Subsequent substitution studies resulted in analogous sulfides with Sm and Gd instead of Nd , while none of the corresponding selenides (or tellurides) could be prepared under the investigated reaction conditions. This contribution introduces the new sulfides $\text{TlLnAg}_2\text{S}_3$, in comparison to $\text{Tl}_2\text{NdAg}_3\text{Se}_4$ and $\text{BaLnAg}_3\text{S}_3$ [15]. For related

quaternary chalcogenides with alkali- and alkaline-earth metal atoms instead of thallium atoms, we refer to a review from Ibers [16].

2. Experimental section

2.1. Synthesis and analysis

The quaternary sulfides were synthesized using the solid state reaction method by mixing the elements Tl , Ln ($\text{La}, \text{Pr}, \text{Nd}, \text{Sm}, \text{Gd}$), Ag , and S in 1: 1: 2: 3 ratio. The elements were stored in an argon-filled glove box (Tl granules, 6 mm, 99.99%; La powder, −40 mesh, 99.9%; Nd powder, −40 mesh, 99.9%; Pr powder, −40 mesh, 99.9%; Sm powder, −40 mesh, 99.9%; Gd powder, −40 mesh, 99.9% (all from Alfa Aesar); S powder, 99.98%, Sigma-Aldrich), and were used as they were purchased. The mixtures were placed into graphite crucibles, which were jacked inside silica tubes and then sealed under dynamic vacuum between 10^{-3} and 10^{-4} mbar. The mixture were heated in a resistance furnace at 750 °C for 24 h and then cooled slowly - past the melting point of the target - to 400 °C over a period of 130 h. Thereafter the furnace was switched off to accelerate the final cooling step.

The phase identification was performed utilizing the INEL powder diffractometer with position-sensitive detector and $\text{Cu-K}\alpha_1$ radiation. The powder diagrams of the ground samples were collected at room temperature for 10–20 min in the 2θ range of 5–120°. A comparison with the simulated pattern obtained from the single crystal structure solution revealed the existence of at minimum minor side products, necessitating further annealing at 450 °C for three weeks. The resulting

* Corresponding author.

E-mail address: kleinke@uwaterloo.ca (H. Kleinke).

X-ray patterns showed that the desired compound $\text{TlLnAg}_2\text{S}_3$ formed as pure phases for $\text{Ln} = \text{Nd}, \text{Sm}$ and Gd , but only as minor products in case of $\text{Ln} = \text{La}$ and Pr .

2.2. Single crystal studies

Single crystal X-ray studies of the three lanthanide sulfides $\text{TlLnAg}_2\text{S}_3$ with $\text{Ln} = \text{Nd}, \text{Sm}, \text{Gd}$, were carried out using Bruker Kappa CCD Apex II diffractometer at room temperature utilizing Mo-K α radiation. The block-like shaped, orange/yellow crystals were selected under an optical microscope and attached to a very thin glass fiber via epoxy. After the determination of the preliminary unit cells, the data were collected by scanning ω and ϕ of 0.3° in different sets of frames for full data coverage and low redundancy, using the search collection strategy part of the APEX II suite. The exposure time was between 10 and 30 s per frame. The data were corrected for Lorentz and polarization effects, then the absorption corrections were applied to the data using the empirical multi-scan method SADABS, part of the APEX II software [17], since the crystal faces could not be determined reliably for numerical absorption corrections.

The systematic absences pointed toward the centrosymmetric $Pnma$ and non-centrosymmetric $Pna2_1$ space groups. The structures were solved in the centrosymmetric $Pnma$ space group using direct method and refined using the least square part of the SHELXTL package [18]. The Platon program [19] was used to standardize the atomic positions via the tidy routine. Crystallographic data are summarized in Table 1, and the atomic positions and equivalent displacement factors of $\text{TlNdAg}_2\text{S}_3$ listed in Table 2. Further details of the crystal structure investigation can be obtained from the Fachinformationszentrum Karlsruhe, 76344 Eggenstein-Leopoldshafen, Germany, (fax: (49) 7247-8 08-666; e-mail: crysdata@fiz-karlsruhe.de) on quoting the depository numbers CSD-433316 ($\text{TlNdAg}_2\text{S}_3$), CSD-433317 ($\text{TlGdAg}_2\text{S}_3$), and CSD-433318 ($\text{TlSmAg}_2\text{S}_3$).

Table 1
Crystallographic details of $\text{TlLnAg}_2\text{S}_3$.

Formula	$\text{TlNdAg}_2\text{S}_3$	$\text{TlSmAg}_2\text{S}_3$	$\text{TlGdAg}_2\text{S}_3$
Formula Weight	660.54	666.66	673.55
Crystal System	orthorhombic	orthorhombic	orthorhombic
Space group	$Pnma$ (No. 62)	$Pnma$ (No. 62)	$Pnma$ (No. 62)
a, b, c [Å]	13.8141(3), 4.1649(1), 11.4008(2)	13.8295(4), 4.1296(1), 11.3443(3)	13.8731(6), 4.0946(2), 11.2999(5)
V [Å ³]	655.94(2)	647.88(3)	641.89(5)
Z	4	4	4
Density [g cm ⁻³]	6.689	6.835	6.970
Absorption coefficient [mm ⁻¹]	38.977	40.511	42.073
$F(000)$	1132	1140	1148
Crystal Size [mm]	0.15 × 0.04 × 0.02	0.04 × 0.04 × 0.02	0.05 × 0.02 × 0.02
Temperature (K)	296	296	296
Radiation [Å]	0.71073	0.71073	0.71073
Total, Unique Data, $R(\text{int})$	4522, 1077, 0.015	4170, 889, 0.022	3898, 1005, 0.020
Observed Data [$I > 2\sigma(I)$]	1020	773	879
Number of reflections, parameters	1077, 44	889, 44	1005, 44
$R(F_o),^a R_w(F_o^2),^b$	0.021, 0.045,	0.022, 0.038,	0.024, 0.050,
GOF (obs. Data)	1.07	1.04	1.05
Min., max. residual electron density [e Å ⁻³]	-2.26, 2.47	-2.00, 1.57	-2.04, 1.87

^a $R(F_o) = \Sigma ||F_o| - |F_c|| / \Sigma |F_o|$.

^b $R_w(F_o^2) = [\Sigma [w(F_o^2 - F_c^2)^2] / \Sigma [w(F_o^2)^2]]^{1/2}$, with F_o and F_c being the observed and calculated structure factors, respectively.

Table 2

Fractional atomic coordinates and equivalent isotropic displacement parameters (Å²) of $\text{TlNdAg}_2\text{S}_3$.

	x	y	z	$U_{eq}/\text{Å}^2$
Tl1	0.26921(2)	1/4	0.54262(3)	0.0283(1)
Nd1	0.47907(2)	1/4	0.83733(3)	0.01109(9)
Ag1	0.03650(5)	1/4	0.08873(5)	0.0282(2)
Ag2	0.32531(4)	1/4	0.27193(5)	0.0300(2)
S1	0.14404(11)	1/4	0.26868(14)	0.0142(3)
S2	0.40261(10)	1/4	0.06771(13)	0.0117(3)
S3	0.58878(12)	1/4	0.62742(13)	0.0156(4)

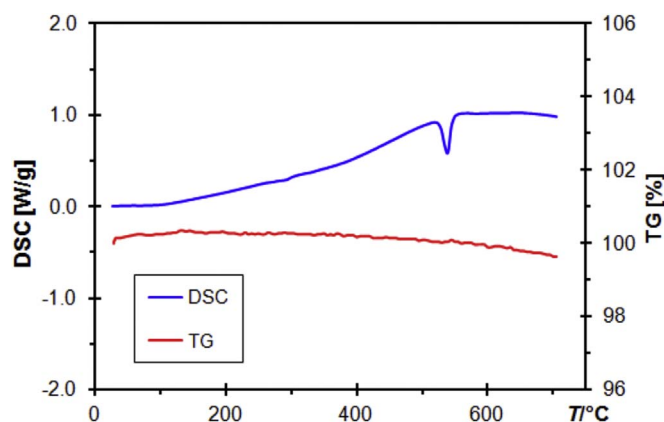


Fig. 1. DSC and TG of $\text{TlNdAg}_2\text{S}_3$.

2.3. Differential scanning calorimetry and thermogravimetry

The thermal behavior of $\text{TlNdAg}_2\text{S}_3$ was investigated by differential scanning calorimetry (DSC) and thermogravimetry (TG) using NETZSCH STA 409 PC Luxx instrument. The experiment was carried out under constant argon flow with a heating rate of $20^\circ\text{C}/\text{min}$ up to 800°C using a sapphire as reference sample. The heating curve revealed an endothermic peak at 540°C , indicating the melting point of this compound, occurring with a weight loss of less than 2% (Fig. 1). An X-ray diagram obtained after the measurement showed only the presence of $\text{TlNdAg}_2\text{S}_3$, consistent with no decomposition; therefore the melting point is a congruent one.

2.4. Electronic structure calculation

The density functional theory (DFT) was employed to calculate the electronic structure of $\text{TlNdAg}_2\text{S}_3$, utilizing the full potential linearized augmented plane wave method (LAPW) embedded in the WIEN2k package [20]. The LSDA+ U method (LSDA: local spin density approximation) [21] was chosen with the standard value of $U = 7$ eV for f elements [22] for the on-site Coulomb interaction of the Nd atoms, and radii of RMT = 2.5 a.u. for all metal atoms and 2.12 a.u. for all sulfur atoms. The spin-polarized calculation was performed with 120 independent k points of the first Brillouin zone on a grid of $6 \times 20 \times 7$ k points along the respective vectors of the reciprocal lattice, with the convergence criterion of the energy change being below 0.0001 Ry.

3. Results and discussion

The new isostructural $\text{TlLnAg}_2\text{S}_3$ structures adopt the space group $Pnma$, where all the atoms are located on the mirror plane (Wyckoff position 4c). The $\text{TlNdAg}_2\text{S}_3$ structure consists of AgS_4 tetrahedra, which share corners and edges to form a three-dimensional network. The channels of this network are filled by Tl and Nd atoms (Fig. 2, left). The condensation of the AgS_4 tetrahedra chains results in the formation of a Ag ribbon with Ag–Ag contacts of 3.07 Å and 3.32 Å (Fig. 2,

Download English Version:

<https://daneshyari.com/en/article/5153329>

Download Persian Version:

<https://daneshyari.com/article/5153329>

[Daneshyari.com](https://daneshyari.com)